frontiers in Energy Research

ORIGINAL RESEARCH
published: 26 May 2021
doi: 10.3389/fenrg.2021.657007

Raman Spectroscopic Study on a CO_2-CH_4-N_2 Mixed-Gas Hydrate System

Liu Chuanhai[1,2], *Chen Ran*[1,2], *Zhang Baoyong*[1,2]*, *Wu Qiang*[1,2], *Zhang Qiang*[1,2], *Gao Xia*[2,3] *and Wu Qiong*[1,2]

[1]Department of Safety Engineering, Heilongjiang University of Science and Technology, Harbin, China, [2]National Central Laboratory of Hydrocarbon Gas Transportation Pipeline Safety, Harbin, China, [3]School of Architecture and Civil Engineering, Heilongjiang University of Science and Technology, Harbin, China

Accurate determination of the characteristics of coal mine gas separation products is the key for gas separation applications based on hydrate technology. Gas hydrates are synthesized from gases with two types of compositions (CO_2-CH_4-N_2). The separation products were analyzed by *in situ* Raman spectroscopy. The crystal structure of the mixed-gas hydrate was determined, and the cage occupancy and hydration index were calculated based on the various vibrational modes of the molecules according to the "loose cage-tight cage" model and the Raman band area ratio combined with the van der Waals-Platteeuw model. The results show that the two mixed-gas hydrate samples both have a type I structure. Large cages of mixed-gas hydrate are mostly occupied by guest molecules, with large cage occupancies of 98.57 and 98.52%; however, small cages are not easy to occupy, with small cage occupancies of 29.93 and 33.87%. The average cage occupancies of these two hydrates are 81.41 and 82.36%, and the stability of the crystal structure of the mixed-gas hydrate in the presence of 75% CO_2 is better than that of the mixed-gas hydrate in the presence of 70% CO_2. The hydration indices of the two hydrate gas samples are 7.14 and 6.98, which are greater than the theoretical value of structure I.

Keywords: gas hydrate, Raman spectra, crystal structure, cage occupancy, hydration index

OPEN ACCESS

Edited by:
Greeshma Gadikota,
Cornell University, United States

Reviewed by:
Jean-Michel Pereira,
École des ponts ParisTech (ENPC), France
Bei Liu,
China University of Petroleum, China

***Correspondence:**
Zhang Baoyong
zhangbaoyong2017@outlook.com

Specialty section:
This article was submitted to Carbon Capture, Storage, and Utilization, a section of the journal Frontiers in Energy Research

Received: *22 January 2021*
Accepted: *11 May 2021*
Published: *26 May 2021*

Citation:
Chuanhai L, Ran C, Baoyong Z, Qiang W, Qiang Z, Xia G and Qiong W (2021) Raman Spectroscopic Study on a CO_2-CH_4-N_2 Mixed-Gas Hydrate System. Front. Energy Res. 9:657007. doi: 10.3389/fenrg.2021.657007

INTRODUCTION

Methane is the main component of coal mine gas in outburst-prone coal seams in China, but there are still many coal seams that mainly contain carbon dioxide, such as the Yaojie coal field in Gansu, the Yingcheng coal field in Jilin, and the Helong coal field (Li et al., 2011; Wang et al., 2009; Shu-Gang et al., 2000). However, due to the complex behaviors of gas mixtures and the lack of separation and utilization technologies suitable for the high concentrations of carbon dioxide in coal mine gas, the carbon dioxide extracted from outburst-prone coal seams is directly discharged into the atmosphere. Studies have shown that (Wu et al., 2009; Wu and Zhang, 2010; Wu et al., 2009) gas hydrates have three advantages: mild formation conditions (2–6 MPa, 0–10°C), a high gas fraction (specifically, 1 m^3 of hydrate contains approximately 160–210 m^3 of coal mine gas in a standard environment), and good storage stability and safety (stable storage in the range of −15 to −10°C at atmospheric pressure). Herein, this project proposes a new method for the separation and storage of high concentrations of carbon dioxide in coal mine gas (Wu et al., 2009). Water molecules serve as a crystal host framework that is stabilized by the inclusion of suitably sized guest molecules. There are

three well-known hydrate structures (Ripmeester et al., 1987; Sloan and Koh, 2008): cubic structure I, cubic structure II and hexagonal structure H. The ideal formulas for cell structures are $8M{\cdot}46H_2O$, $24M{\cdot}136H_2O$, and $6M{\cdot}34H_2O$ (where M stands for molecules). The formula of the hydrate crystal cell structure can be written more generally as $mM{\cdot}nH_2O$ (where n is the hydration index). The results showed that gas hydrates are nonstoichiometric crystalline inclusion compounds; therefore, the key indicators for high concentrations of carbon dioxide in coal mine gas hydrate separation products are crystal structure, cage occupancy and hydration index.

However, the analysis of hydrate characteristics has been conducted only at the macroscopic scale to date, and some parameters are determined by temperature and pressure change rates. It is difficult to observe microscopic details after hydrate formation (Li et al., 2008; Li et al., 2012). With the progress in modern analytical methods, Raman spectroscopy (Raman), nuclear magnetic resonance (NMR) spectroscopy, X-ray diffraction (XRD), and other precision analytical methods have been widely used to study gas hydrates (Uchida et al., 2003; Yoon et al., 2004; Lu et al., 2007), making it is possible to observe the microscopic characteristics of hydrates and allowing research to be more detailed and accurate.

In micro laser Raman spectroscopy (MLRM), the incident light is focused on a sample through a microscope, yielding various Raman spectral information such as chemical composition, crystal structure, molecular interactions, and molecular orientations without interference from the surrounding material. Micro laser Raman spectroscopy has been widely used in various fields (Lin-Tao et al., 2007; Qin et al., 2007a,b; Burke, 2001; Hong-Rui et al., 2003; Wang and Yang, 2007; Liu et al., 2007; Liu et al., 2007). In recent years, domestic and international scholar have successfully applied it to study pure CH_4, pure H_2, pure CO_2 hydrate and binary systems, and it has certain advantages for the study of hydrate crystal microparameters (Susilo et al., 2007; Luzi et al., 2012; Huang et al., 2020). Liu Chang-ling et al. (Liu et al., 2010) used a laser Raman spectrometer to calculate the corresponding hydration index and cage occupancy for an aqueous sodium dodecyl sulfate (SDS)-methane system, a powder ice-methane system and a sand-methane system consisting of sand with different particle sizes. Sum et al. (Sum et al., 1997) studied the methane hydrate structure and reported that methane gas fills 5^{12} cages to form cage structures. Uchida et al. (Uchida et al., 1996) measured the density of CH_4 and CO_2 guest molecules by the Raman spectroscopy method. Alondra Torres Trueba et al. (Trueba et al., 2012) applied laser *in situ* observations of H_2-TBAB hydrate to study the security of hydrogen storage and transportation. Yuya Hiraga et al. (Hiraga et al., 2019) analyzed the cage occupancy of thin homogeneous methane hydrate (MH) films at 2.9–7.6 MPa and 273–276 K. The MH films were synthesized on the lower surface of a sapphire window of a high-pressure cell to eliminate the noise associated with C-H stretching vibrations of bulk methane gas. Intermediate to small cage occupancy ratios were determined for the MH films to assess the reliability of the deconvolution functions used in data reduction. Hiroyuki Komatsu et al. analyzed methane clathrate hydrate dissociation with Raman spectroscopy and a thermodynamic mass transfer model to determine cage occupancy (Komatsu et al., 2019). The kinetics of methane and methane/propane hydrate formation/dissociation were investigated (Truong-Lam et al., 2020). The results of an *in situ* Raman analysis revealed that methane and methane/propane hydrates showed different spectral features for the O-H stretching band depending on the gas hydrate structure type (Truong-Lam et al., 2018). Spectroscopic analysis of a multivariate hydrate system is relatively limited, and there are currently no reports on Raman spectroscopic analysis of high CO_2 concentrations in mixed-gas hydrates.

Herein, the author simulated a high-pressure and low-temperature environment with a self-developed cell with a metal jacket and a sapphire window to synthesize a CO_2-CH_4-N_2 mixed-gas hydrate, analyzed the crystal structure of the hydrate separation product, and calculated the cage occupancy and hydration index.

EXPERIMENTAL SECTION

Equipment and Materials

The experimental apparatus consisted of a laser Raman spectrometer, a gas supply system, a jacketed cooling-type high-pressure visual cell, a temperature control system, a data acquisition system and other parts. A high-precision Lab RAM HR-800 type visible confocal Raman microscope (JY Company, France) was used to study the gas hydrates and was equipped with an automatic platform, an open confocal microscope system with a spatial resolution of <1 μm in the horizontal direction and <2 μm in the vertical direction, a 785 and 532 nm laser, 1800 lines/mm and 600 lines/mm gratings and a 50× telephoto lens. In addition, to characterize the products of high-CO_2 mixed-gas hydrate gas separation, nondestructive and accurate measurements were made by means of an independently designed cooled-jacket *in situ* high-pressure reactor with a sapphire window to ensure full transparency of the laser and a visual reactor with an effective volume of 3 ml at a compression of 20 MPa. A photograph of the *in situ* Raman spectroscopy test apparatus in which the mixed-gas hydrate separation products were characterized is shown in **Figure 1**.

Sample Preparation and *In Situ* Raman Spectroscopic Analysis

Sample Preparation

CO_2-CH_4-N_2 mixed-gas hydrates were synthesized in a high-pressure cell with a 3 ml capacity and a sapphire window with a diameter of 1.5 cm. The evacuated cell was half-filled with deionized water, and the reaction kettle was cleaned two to three times by the same gas sample. The experimental reactor temperature decreased to 1°C and remained stable, and then the reaction kettle was filled with gas to a pressure of 5 MPa. The specific initial conditions are shown in **Table 1**. When the experiment lasted 6 min, the sample in the experimental reactor at the gas-water interface appeared as a white granular

FIGURE 1 | Apparatus for hydrate measurements using *in situ* Raman spectroscopy.

TABLE 1 | The initial conditions for hydrate synthesis.

Gas	Initial pressure P/MPa	Initial temperature T/°C	Vapor-liquid ratio
1 (70%CO_2+16%CH_4+14%N_2) 2 (75%CO_2+11%CH_4+14%N_2)	5	1	75

FIGURE 2 | Typical photos of the hydrate formation process.

hydrate, as shown in **Figure 2A**, and the pressure decreased to 4.17 MPa. After refrigeration for 28 min, a white hydrate area appeared along the reactor wall and the reaction kettle windows; this hydrate area continued to grow, gradually blurring the initially transparent experiment kettle windows and reducing visibility in the kettle, as shown in **Figure 2B**. As the hydration reaction continued for 75 min, a white snow-like hydrate nearly filled the whole cell; the hydrate gas pressure no longer changed, indicating that the hydration reaction had reached equilibrium and that hydrate formation had ended, as shown in **Figure 2C**. Raman *in situ* analysis was performed after 3–5 days.

In Situ Raman Spectroscopic Analysis

A laser Raman spectrometer was used to analyze a silicon sample, with an excitation wavelength of 532 nm, a power of 40 mW, a spectral acquisition range of 1000–3100 cm^{-1}, and an integration time of 40 s. At total of four scans were accumulated. The experimental data in this article is the average data obtained through repeated experiments of three measurements.

RESULTS AND DISCUSSION

Analysis of Crystal Structure

Raman spectra of the guest gas provide important information about the hydrate structure, the mechanism of hydrate formation/decomposition, the cage occupancy, the hydration index, the composition of the hydrates and the molecular dynamics. The hydrate structure can be determined by comparing Raman data or comprehensively considering other spectral information. **Figures 3A,B** show the Raman spectra of mixed-gas hydrates with CO_2 concentrations of 70 and 75%, respectively. The information obtained by the Raman spectra is shown in **Table 2**.

According to the hydrate "loose cage-tight cage" model (Subramanian and Sloan, 2002), in a "loose cage"—CH_4 molecules captured in a large cage—the C-H stretching frequency compared with that of free CH_4 gas molecules has an obvious blueshift. In a "tight cage"—CH_4 molecules in a small cage—the C-H stretching frequency approaches that of free CH_4 gas molecules. The frequencies of CH_4 molecules in the large cage

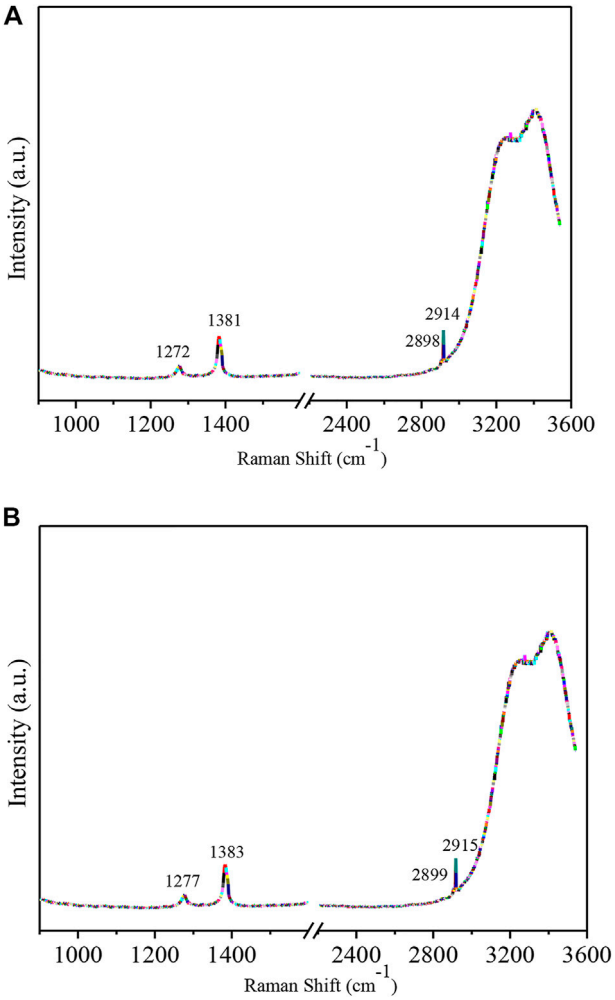

FIGURE 3 | (A) Raman spectra of 70% CO_2 mine mixed-gas hydrates. **(B)** Raman spectra of 75% CO_2 mine mix8lJed-gas hydrates.

were 2898 cm^{-1} and 2899 cm^{-1}, and the frequencies of CH_4 molecules in the small cage were 2914 cm^{-1} and 2915 cm^{-1}.

To date, the study of CO_2-CH_4 mixed hydrates has been limited, and in order to confirm that CO_2 is occupying the hydrate small cage? The author made the following three assumptions regarding the hydrate in gas sample 1: 1) the frequencies of CO_2 molecules occupying large cages were 1272 cm^{-1} and 1381 cm^{-1}; 2) the frequencies of the CO_2 molecules occupying large cages and small cages were 1272 cm^{-1} and 1381 cm^{-1}, respectively; 3) the frequencies of the CO_2 molecules occupying small cages and large cages were 1272 cm^{-1} and 1381 cm^{-1}, respectively. The same assumptions were also made for the hydrate of sample 2. The author determined that the ratio of the Raman peak areas of the large cage and the small cage was approximately 3:1 when the Raman shifts of 1272 cm^{-1},1381 cm^{-1}, 1277 cm^{-1} and 1383 cm^{-1} attributed to the CO_2 stretching and bending vibrations

TABLE 2 | The information provided by Raman spectroscopy.

Gas	Raman shift/P (cm^{-1})	Raman area
1	1272	329.4
	1381	512.5
	2898	248.1
	2914	327.0
2	1277	310.3
	1383	526.6
	2899	389.5
	2915	420.3

corresponded to CO_2 molecules captured in large cages. Other assumptions regarding structure I or II hydrates were not satisfied; rather the results indicated that the two CO_2 and CH_4 mixed-gas hydrate samples under a pressure of 5 MPa and an initial temperature of 1°C and were both structure I hydrates.

The Raman shifts of 1272 cm^{-1} and 1381 cm^{-1} were attributed to the stretching and bending vibrations of CO_2 molecules in large cages, and the frequencies of CH_4 molecules in large cages and small cages were 2898 cm^{-1} and 2914 cm^{-1}, respectively, for structure 1 hydrates. The Raman shifts of 1277 cm^{-1} and 1383 cm^{-1} were attributed to the stretching and bending vibrations of CO_2 molecules in large cages, and the frequencies of CH_4 molecules in large cages and small cages were 2899 cm^{-1} and 2915 cm^{-1}, respectively, for structure 2 hydrate. As the CO_2 concentration increased, the CH_4 concentration decreased, and the Raman shift of the mixed-gas hydrates varied.

Calculations of the Age Occupancy and Hydration Index

The ratio of the Raman spectral band area of the small cage to that of the large cage can be combined with a statistical thermodynamics equation to calculate the hydrate cage occupancy and hydration index (Ripmeester and Ratcliffe, 1988; Uchida et al., 2004; Lu et al., 2005; Hester et al., 2007; Lu et al., 2007). The number of large cages is three times that the number of small cages in a structure I hydrate; as a result, the occupancy of large cages should be greater than the total object number of molecules in small cages. Correspondingly, the band areas reflect the guest molecule occupancy of the two cage sizes. The ratio of the guest gas occupancy in a large cage to that in a small cage can be calculated by using the following formula.

$$\frac{\theta_L}{\theta_S} = \frac{I_L}{3I_S} \tag{1}$$

where θ_L and θ_S are the absolute cage occupancies in the large cage and small cage, respectively, and I_L and I_S are the Raman peak areas for the large cage and small cage, respectively.

The calculation for a multiple-occupancy hydrate cage system is similar to that of a pure gas hydrate. CH_4 and CO_2 mixed-gas hydrates were synthesized in the two experiments, and the CH_4

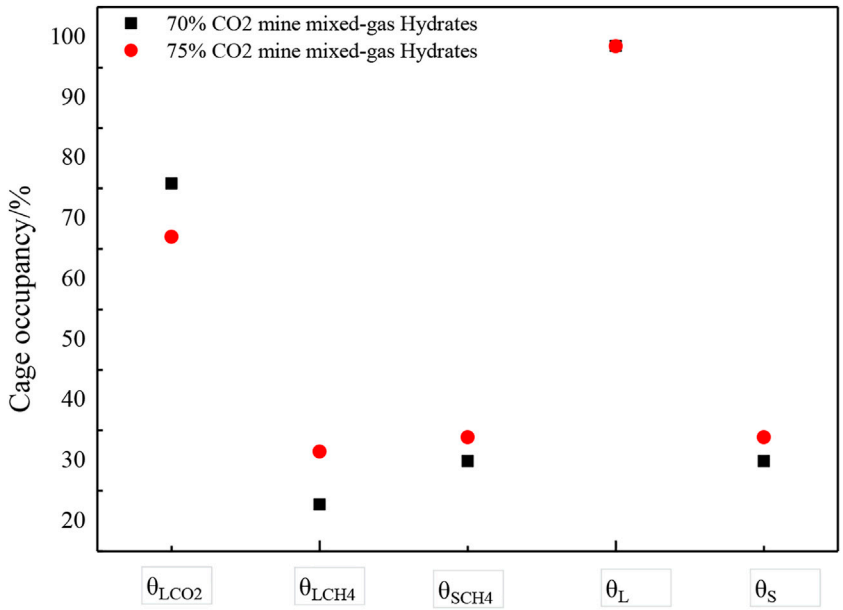

FIGURE 4 | Cage occupancy of hydrates.

and CO_2 relative occupancies, $\theta_{S,CH_4}/\theta_{S,CO_2}$, $\theta_{L,CH_4}/\theta_{L,CO_2}$, $\theta_{L,CH_4}/\theta_{S,CH_4}$, and $\theta_{L,CO_2}/\theta_{S,CO_2}$, were calculated by deconvolution of the Raman spectra. The van der Waals and Platteeuw hydrate statistical thermodynamic model was used to determine the CO_2 and CH_4 cage occupancies in the large and small cages, and the method for calculating the cage occupancy is similar to that for a pure gas hydrate.

$$\Delta\mu_{W,H} = -\frac{RT}{23}\left[3\ln\left(1-\theta_{L,CO_2}-\theta_{L,CH_4}\right)+\ln\left(1-\theta_{S,CO_2}-\theta_{S,CH_4}\right)\right] \tag{2}$$

$$\Delta\mu_{W,H} = \Delta\mu_{W,L} \tag{3}$$

When the gas, water, and hydrate phases are in equilibrium, the chemical potential difference $\Delta\mu_{W,H}$ of molecules in the empty crystal lattice of the structure I hydrate usually takes a value of 1297 $j.mol^{-1}$[(Lei et al., 2005)]. This value was calculated with **Eqs 2**, **3** combined with the occupancies of CO_2 and CH_4 in the large and small cages, $\theta_{S,CH_4}/\theta_{S,CO_2}$, $\theta_{L,CH_4}/\theta_{L,CO_2}$, $\theta_{L,CH_4}/\theta_{S,CH_4}$, and $\theta_{L,CO_2}/\theta_{S,CO_2}$.

The formula for calculating the hydration index is as follows:

$$n = \frac{23}{3\theta_{L,CO_2}+3\theta_{L,CH_4}+\theta_{S,CO_2}+\theta_{S,CH_4}} \tag{4}$$

The peak areas of the large cage and the small cage can be determined from the cage occupancy by applying Raman integration software, as shown in **Figure 4**. In gas 1, $\theta_{L,CH_4}/\theta_{L,CO_2} = 0.3$ and, $\theta_{L,CH_4}/\theta_{S,CH_4} = 0.76$. In gas 2, $\theta_{L,CH_4}/\theta_{L,CO_2} = 0.47$ and $\theta_{L,CH_4}/\theta_{S,CH_4} = 0.93$. According to **Eqs. 2–4**, for a CO_2 concentration of 70%, the mixed-gas hydrate cage occupancies were $\theta_{L,CO_2} = 75.82\%$, $\theta_{S,CH_4} = 29.93\%$, and $\theta_{L,CH_4} = 22.75\%$; the large cage occupancy reached 98.57%, the small cage occupancy reached 29.93%, and the hydration index was 7.14. For a CO_2 concentration of 75%, the mixed-gas hydrate cage occupancies were $\theta_{L,CO_2} = 67.02\%$, $\theta_{S,CH_4} = 33.87\%$, and $\theta_{L,CH_4} = 31.50\%$; the large cage occupancy reached 98.52%, the small cage occupancy reached 33.87%, and the hydration index was 6.98. In both cases, the values are greater than the theoretical value for a structure I hydration index. Large cages of mixed-gas hydrates are mostly filled by guest molecules, whereas only a few CH_4 molecules occupy small cages. When the CO_2 concentration in the mixed gas is higher, the CO_2 occupancy of the large cage is much larger than the CH_4 occupancy. Analyses showed that the ability of a guest gas to fill large and small cages is positively related to its concentration under the given temperature and pressure conditions.

Analysis of the Average Cage Occupancy

To some degree, the stability of the whole crystal structure depends on the cage occupancy. When more hydrate crystal cages were occupied by guest molecules, the hydrate crystal structure was more stable. The average cage occupancy was computed by **Eq. 5**. When the CO_2 concentration was 70% of the mixed-gas hydrate, and the average cage occupancy was $\theta_A = 81.41\%$. When the CO_2 concentration was 75% of the mixed-gas hydrate, the average cage occupancy was $\theta_A = 82.36\%$. It follows that the stability of the crystal structure with a CO_2 concentration of 75% of the mixed-gas hydrate was better than that of the structure with a CO_2 concentration of 70%.

$$\theta_A = \frac{3\theta_L+\theta_s}{4} \tag{5}$$

Marisa (Rydzy et al., B2007) showed that CH_4 molecules are known to occupy small as well as large cages of structure I hydrates, whereas CO_2, in general only occupies the large

cavities in this structure. the guest-to-cavity size ratios for the methane and carbon dioxide molecules indicate that CO_2 (0.834) stabilizes the large cage better than CH_4 (0.744). it can be concluded that the more CO_2 molecules are encaged in the large cages of the sI hydrate lattice instead of CH_4, the more stable the lattice becomes. In this work, To some degree, When the CO_2 concentration was 70% of the mixed-gas hydrate, the average cage occupancy was θA = 81.41%. When the CO_2 concentration was 75% of the mixed-gas hydrate, the average cage occupancy was θA = 82.36%. It follows that the stability of the crystal structure with a CO_2 concentration of 75% of the mixed-gas hydrate was better than that of the structure with a CO_2 concentration of 70%. Consequently, the stability of CO_2-CH_4 hydrates might reach a maximum when all of the large cavities are filled with CO_2.

CONCLUSION

Analysis shows that CO_2 and CH_4 formed mixed-gas hydrates under a pressure of 5 MPa and an initial temperature of 1°C; at the same time, the mixed-gas hydrates were both structure I hydrates. As the CO_2 concentration increased and the CH_4 concentration decreased, the Raman shift of mixed-gas hydrate change slightly.

The occupancies of the large cages of two mixed-gas hydrates were 98.57 and 98.52%, while the occupancies of the small cages were 29.93 and 33.87%. The results showed that the large cages of the mixed-gas hydrates were easily filled by guest molecules, while the small cages were not, and the stability of the crystal structure at a CO_2 concentration of 75% of the mixed-gas hydrate was better than that at a CO_2 concentration of 70%. The hydration indices were 7.14 and 6.98, which are greater than the theoretical value of 5.75. Calculating the cavity occupancy and hydration index of mixed-gas hydrates is a good method to understand the structure and mechanism of formation of the mixed-gas hydrates. Knowledge of the different subcomponent systems and filling process of gas hydrates, as well as the structure types and resources, is of significance. At the same time, this study will support the idea of methane exploitation in linkage with CO_2 isolation (Ohgaki et al., 1996).

DATA AVAILABILITY STATEMENT

The original contributions presented in the study are included in the article/Supplementary Material, further inquiries can be directed to the corresponding author.

AUTHOR CONTRIBUTIONS

LC: Thesis writing; CR: The data processing; ZB: Writing guidance; WQa: The experiment design; ZQ: The data analysis; GX: The data analysis; WQo: The data analysis.

ACKNOWLEDGMENTS

The work reported in this paper was funded by the National Natural Science Foundation of China under NSFC Contract No. 51704103, 51774123, 51974112, 51804105.

REFERENCES

Burke, E. A. J. (2001). Raman Microspectrometry of Fluid Inclusions. *Lithos* 55, 139–158. doi:10.1016/s0024-4937(00)00043-8

Hester, K. C., Dunk, R. M., White, S. N., Brewer, P. G., Peltzer, E. T., and Sloan, E. D. (2007). Gas Hydrate Measurements at Hydrate Ridge Using Raman Spectroscopy. *Geochimica et Cosmochimica Acta* 71, 2947–2959. doi:10.1016/j.gca.2007.03.032

Hiraga, Y., Sasagawa, T., Yamamoto, S., Komatsu, H., Ota, M., Takao, T., et al. (2019). A Precise Deconvolution Method to Derive Methane Hydrate Cage Occupancy Ratios Using Raman Spectroscopy. *Chem. Eng. Sci.* 214, 115361. doi:10.1016/j.ces.2019.115361

Hong-Rui, F., Tao, K. J., Xie, Y. H., and Wang, K. Y. (2003). Laser Raman Spectroscopy of Typical Rare-Earth Fluoro-Carbonate Minerals in Bayan Obo REE-Fe-Nb deposit and Identification of Rare-Earth Daughter Minerals Hosted in Fluid Inclusions. *Acta Petrologioa Sinica* 19 (1), 169–172.

Huang, X., Cai, W., Zhan, L., and Lu, H. (2020). Study on the Reaction of Methane Hydrate with Gaseous CO2 by Raman Imaging Microscopy. *Chem. Eng. Sci.* 222, 115720. doi:10.1016/j.ces.2020.115720

Komatsu, H., Sasagawa, T., Yamamoto, S., Hiraga, Y., Ota, M., Tsukada, T., et al. (2019). Methane Clathrate Hydrate Dissociation Analyzed with Raman Spectroscopy and a Thermodynamic Mass Transfer Model Considering Cage Occupancy. *Fluid Phase Equilibria* 489, 41–47. doi:10.1016/j.fluid.2019.02.004

Lei, H., Guan, B., Jian-hui, L., and Li, Z. (2005). Coupled Relationship Among Hydrate Structure, Hydration Number, and Raman Spectrum. *Geo Sci.* 19 (1), 83–88. doi:10.3969/j.issn.1000-8527.2005.01.012

Li, D., Du, J., He, S., Liang, D., Zhao, X., and Yang, X. (2012). Measurement and Modeling of the Effective Thermal Conductivity for Porous Methane Hydrate Samples. *Sci. China Chem.* 55 (3), 373–379. doi:10.1007/s11426-011-4459-8

Li, W., Cheng, Y. P., and Yun-Feng, Y. (2011). Research on the Genesis and Accumulation of Carbon Dioxide in the Yaojie Coalfield. *J. China Univ. Mining Tech.* 40 (2), 190–195.

Li, X.-S., Zhang, Y., Li, G., Chen, Z.-Y., Yan, K.-F., and Li, Q.-P. (2008). Gas Hydrate Equilibrium Dissociation Conditions in Porous Media Using Two Thermodynamic Approaches. *The J. Chem. Thermodynamics* 40, 1464–1474. doi:10.1016/j.jct.2008.04.009

Lin-Tao, Y., Mu-hua, L., Dao-jin, L., and Ren-fa, C. (2007). Advances in Inspecting Agricultural Products Quality Using Laser Technology. *Acta Laser Biol. Sinica* 16 (3), 370. doi:10.3969/j.issn.1007-7146.2007.03.022

Liu, C. L., Ye, Y. G., and Meng, Q. G. (2010). [Determination of Hydration Number of Methane Hydrates Using Micro-laser Raman Spectroscopy]. *Guang Pu Xue Yu Guang Pu Fen Xi* 30 (4), 963–966. doi:10.3964/j.issn.1000-0593(2010)04-0963-04

Liu, W.-H., Yang, W., Wu, X.-Q., and Lin, Z.-X. (2007). Direct Determination of Ethanol by Laser Raman Spectra with Internal Standard Method. *Chin. J. Anal. Chem.* 35 (3), 416–418. doi:10.3321/j.issn:0253-3820.2007.03.023

Liu, W.-H., Yang, W., Wu, X.-Q., and Lin, Z.-X. (2007a). Direct Quantitative Determination of Methanol by Laser Raman Spectrometry with Internal Standard Method. *Chin. J. Anal. Chem.* 35 (10), 1503–1505. doi:10.3321/j.issn:0253-3820.2007.10.024

Lu, H., Seo, Y. T., and Lee, J. W. (2007). Complex Gas Hydrate from the Cascadia Margin. *Nature* 445 (18), 303–306. doi:10.1038/nature05463

Lu, H., Moudrakovski, I., Riedel, M., Spence, G., Dutrisac, R., Ripmeester, J., et al. (2005). Occurrence and Structural Characterization of Gas Hydrates Associated

with a Cold Vent Field, Offshore Vancouver Island. *J. Geophys. Res.* 110, B10204. doi:10.1029/2005jb003900

Luzi, M., Schicks, J. M., Naumann, R., and Erzinger, J. (2012). Systematic Kinetic Studies on Mixed Gas Hydrates by Raman Spectroscopy and Powder X-ray Diffraction. *J. Chem. Thermodynamics* 48, 28–35. doi:10.1016/j.jct.2011.12.004

Ohgaki, K., Takano, K., Sangawa, H., Matsubara, T., and Nakano, S. (1996). Methane Exploitation by Carbon Dioxide from Gas Hydrates. Phase Equilibria for CO2-CH4 Mixed Hydrate System. *J. Chem. Eng. Jpn.* 29 (3), 478–483. doi:10.1252/jcej.29.478

Qin, C. J., Qiu, Y. Z., Zhou, G. F., and Wang, Z. G. (2007b). Fluid Inclusion Study of Carbonatite Dykes/veins and Ore-Hosted Dolostone at the Bayan Obo Ore deposit. *Acta Petrologioa Sinica* 23 (1), 161–168. doi:10.3321/j.issn:1000-0569.2007.01.020

Qin, C. J., Qiu, Y. Z., Zhou, G. F., Wang, Z. G., Zhang, T. R., and Xiao, G.W. (2007a). Laser Raman Spectroscopic Analysis of Bayan Obo Carbonatite Dykes and its Petrogenetic Significance. *Acta Minalogica Sinica* 27 (3/4), 400. doi:10.16461/j.cnki.1000-4734.2007.z1.018

Ripmeester, J. A., and Ratcliffe, C. I. (1988). Low-temperature Cross-Polarization/magic Angle Spinning Carbon-13 NMR of Solid Methane Hydrates: Structure, Cage Occupancy, and Hydration Number. *J. Phys. Chem.* 92, 337–339. doi:10.1021/j100313a018

Ripmeester, J. A., Tse, J. S., and Ratcliffe, C. I. (1987). Some Structural Studies of Clathrate Hydrate. *J. de Physique* 114, 2173–2181. doi:10.1051/jphyscol:1987173

Rydzy, M. B., Schicks, J. M., Naumann, R., and Erzinger, J. (2007). Dissociation Enthalpies of Synthesized Multicomponent Gas Hydrates with Respect to the Guest Composition and Cage Occupancy. *J. Phys. Chem. B* 111, 9539–9545. doi:10.1021/jp0712755

Shu-Gang, Li., Chang, X. T., and Jing-Cai, X. (2000). On Key Stratum Team of Shallow Seam. *J. Xi'an Univ. Sci. Tech.* 20 (1), 1–4. doi:10.13800/j.cnki.xakjdxxb.2000.01.002

Sloan, E. D., and Koh, C. H. (2008). *Clatrate Hydrates of Natural Gases*. 3rd Edn. Boca Raton, FL: CRC Press

Subramanian, S., and Sloan, E. D. (2002). Trends in Vibrational Frequencies of Guests Trapped in Clathrate Hydrate Cages. *J. Phys. Chem. B* 106, 4348–4355. doi:10.1021/jp013644h

Sum, A. K., Burruss, R. C., and Sloan, E. D. (1997). Measurement of Clathrate Hydrates via Raman Spectroscopy. *J. Phys. Chem. B* 101, 7371–7377. doi:10.1021/jp970768e

Susilo, R., Ripmeester, J. A., and Englezos, P. (2007). Characterization of Gas Hydrates with PXRD, DSC, NMR and Raman Spectroscopy. *Chem. Eng. Sci.* 62 (15), 3930–3939. doi:10.1016/j.ces.2007.03.045

Trueba, A. T., Radović, I. R., Zevenbergen, J. F., Kroon, M. C., and Peters, C. J. (2012). Kinetics Measurements and *In Situ* Raman Spectroscopy of Formation of Hydrogen-Tetrabutylammonium Bromide Semi-hydrates. *Int. J. Hydrogen Energ.* 37, 5790–5797. doi:10.1016/j.ijhydene.2011.12.053

Truong-Lam, H. S., Seo, S. D., Kim, S., Seo, Y., and Dong, J. (2020). An Iin-Ssitu Raman Study of the Formation and Dissociation Kinetics of Methane and Methane/propane Hydrates. *Energy & Fuels* 34, 6288–6297. doi:10.1021/acs.energyfuels.0c00813

Truong-Lam, H. S., Seo, S. D., Kim, S., Seo, Y., and Dong, J. (2018). *In Situ* Raman Investigation on Mixed CH_4-C_3h_8 Hydrate Dissociation in the Presence of Polyvinylpyrrolidone. *Fuel* 214, 505–511. doi:10.1016/j.fuel.2017.11.063

Uchida, T., Takagi, A., Hirano, T., Narita, H., Kawabata, J., Hondoh, T., et al. (1996). Measurements on Guest-Host Molecular Density Ratio of CO_2 and CH_4 Hydrates by Raman Spectroscopy. Proceedings of the Second International Conference on Natural Gas Hydrates, Toulouse, France, June 2–6, 1996, 335–339. doi:10.1007/BF00729860

Uchida, T., Moriwaki, M., Takeya, S., Ikeda, I. Y., Ohmura, R., Nagao, J., et al. (2004). Two-step Formation of Methane-Propane Mixed Gas Hydrates in a Batch-type Reactor. *Aiche J.* 50 (2), 518–523. doi:10.1002/aic.10045

Uchida, T., Takeya, S., Wilson, L. D., Tulk, C. A., Ripmeester, J. A., Nagao, J., et al. (2003). Measurements of Physical Properties of Gas Hydrates and *In Situ* Observations of Formation and Decomposition Processes via Raman Spectroscopy and X-ray Diffraction. *Can. J. Phys.* 81, 351–357. doi:10.1139/p03-017

Wang, L. J., Sun, D. S., and Zhang, L. R. (2009). Application of In-Situ Stress Measurement on Bursts Disasters of Rock and CO_2 in Coal Mine. *J. China Coal Soc.* 34 (1), 28–32.

Wang, Y., and Yang, Q. (2007). Raman Spectra of Different Done Part of Fossils Dinosaurs. *A Chin. J. Light Scattering* 19 (2), 128. doi:10.13883/j.issn1004-5929.2007.02.006

Wu, Q., Zhang, B. Y., and Sun, D. L. (2009a). Experimental on Mine Gas Separation Based on Hydration Mechanism. *J. China Coal Soc.* 34 (3), 361–365.

Wu, Q., and Zhang, B. Y. (2010). The Effect of THF-SDS on Separation of Methane-Hydrate from Mine Gas. *J. China Univ. Mining Tech.* 39 (4), 484–489.

Wu, Q., Zhu, Y. M., and Zhang, B. Y. (2009b). Effects of Sodium Dodecyl Sulfate and Kaolin on Low-Concentration Mine Gas Hydration Separation. *CIESC* 60 (5), 1193–1198. doi:10.3321/j.issn:0438-1157.2009.05.020

Yoon, J.-H., Kawamura, T., Yamamoto, Y., and Komai, T. (2004). Transformation of Methane Hydrate to Carbon Dioxide Hydrate: *In Situ* Raman Spectroscopic Observations. *J. Phys. Chem. A.* 108, 5057–5059. doi:10.1021/jp049683l

Conflict of Interest: The authors declare that the research was conducted in the absence of any commercial or financial relationships that could be construed as a potential conflict of interest.